Neuro-Oncology 15(12):1652–1663, 2013.
doi:10.1093/neuonc/not118
Advance Access publication October 24, 2013

A miR-297/hypoxia/DGK-α axis regulating glioblastoma survival

Benjamin Kefas†, Desiree H. Floyd†, Laurey Comeau, Alyse Frisbee, Charli Dominguez, Charles G. diPierro, Fadila Guessous, Roger Abounader, and Benjamin Purow

Division of Neuro-Oncology, Neurology Department, University of Virginia Health System, Charlottesville, Virginia

Background. Despite advances in the treatment of the most aggressive form of brain tumor, glioblastoma, patient prognosis remains disappointing. This failure in treatment has been attributed to dysregulated oncogenic pathways, as observed in other tumors. We and others have suggested the use of microRNAs (miRs) as therapeutic tools able to target multiple pathways in glioblastoma.
Methods. This work features PCR quantification of miRs and transient transfection of many glioblastoma cell lines with miRs, followed by cell number analysis, trypan blue staining, alamarBlue assay of cell viability, caspase-3/-7 activity assay, immunoblot of cleaved poly(ADP-ribose) polymerase and fluorescence activated cell sorting and imaging of apoptotic nuclei, cell invasion assays, MRIs of glioblastoma xenografts in mice using transiently transfected cells as well as posttumor treatment with lentiviral vector encoding miR-297, and analysis of miR-297 target diacylglycerol kinase (DGK)–α including immunoblot, 3′UTR luciferase activity, and rescue with DGK-α overexpression. Cell counts and DGK-α immunoblot were also analyzed in the context of hypoxia and with overexpression of heterogeneous ribonucleoprotein L (hnRNPL).
Results. We identified miR-297 as a highly cytotoxic microRNA in glioblastoma, with minimal cytotoxicity to normal astrocytes. miR-297 overexpression reduced in vitro invasiveness and in vivo tumor formation. DGK-α is shown to be a miR-297 target with a critical role in miR-297 toxicity. In addition, hypoxia and its mediator hnRNPL upregulated DGK-α and buffered the cytotoxic effects of miR-297.
Conclusion. This work shows miR-297 as a novel and physiologic regulator of cancer cell survival, largely through targeting of DGK-α, and also indicates that hypoxia ameliorates miR-297 toxicity to cancer cells.
Keywords: apoptosis, cancer, diacylglycerol kinase-alpha, glioblastoma, hypoxia, microRNA-297.

Glioblastoma multiforme (GBM) is the most aggressive primary brain tumor in adults. Despite some progress in treatment, patient prognosis remains very poor. Resistance of tumors to standard therapies arises from a number of factors, including genetic heterogeneity, a multiplicity of genetic lesions, and dysregulated pathways within each tumor.[1,2] This suggests that new targets and approaches are required to combat this devastating disease. We and others have previously reported the potential of microRNAs (miRNAs, or miRs) as potential therapeutic tools able to target multiple oncogenic pathways in tumors such as glioblastoma.[3–12]

MiRNAs belong to a class of noncoding RNAs that represent ∼2% of the eukaryotic transcriptome. They function by regulating protein expression through binding to complementary "seed matches" on the 3′ untranslated regions (UTRs) of their targets.[13,14] They are involved in the coordination of critical cellular processes such as development, differentiation, proliferation, apoptosis, tumorigenesis, and metabolism.[9,10,13,15] MiRNAs originate as hairpins within long primary transcripts, typically several hundred nucleotides long.[16] These transcripts are processed in the nucleus by the ribonuclease Drosha into inactive precursor pre-miRNAs that are ∼70 nucleotides long.[13–16] The export of the pre-miRNA to the cell cytosol allows for its processing by the enzyme Dicer into an active 19–23 nucleotide miRNA. The resultant active miRNA is incorporated into the RNA-induced silencing complex, where it directs target mRNA translational inhibition or degradation.[13–16] MiRNAs negatively regulate numerous genes, suggesting their potential as therapeutic tools for the treatment of cancers with multiple dysregulated oncogenic pathways.[17]

Hypoxia is another factor that plays a key role in the survival of glioblastoma and other tumors, including their adaptation to hostile microenvironments and resistance to treatment. These effects of hypoxia are believed

Received July 20, 2013; accepted July 7, 2013.

†These authors contributed equally to this work.

Corresponding Authors: Benjamin Kefas, B. Pharm, MSc, PhD, University of Virginia Health System, Old Medical School, Rooms 4885/4881, 21 Hospital Drive, Charlottesville, VA 22908 (bak4x@virginia.edu); Benjamin Purow, MD, University of Virginia Health System, Old Medical School, Rooms 4885/4881, 21 Hospital Drive, Charlottesville, VA 22908 (bwp5g@virginia.edu).

to occur through the induction of metabolic and transcriptional factors,[8,18–24] with both transcriptional and posttranscriptional activation mechanisms contributing to the oncogenic effects of hypoxia. A recent study has also suggested another oncogenic function of hypoxia as a modulator of microRNA function.[25]

To identify new miRs with tumor-suppressive properties, we tested several oncogene-downregulated miRs and identified miR-297 as the most cytotoxic in glioblastoma. Herein, we report that forced expression of miR-297 decreased survival, invasiveness, and tumorigenicity of glioblastoma lines, targeting diacylglycerol kinase (DGK)–α, with minimal effect on normal astrocytes. We report 2 in vivo xenograft assays of glioblastoma tumor growth reduced by both miR-297 transient transfection and a miR-297–encoding lentiviral transduction of established GBM stem cell tumors. Also, hypoxia and its mediator heterogeneous ribonucleoprotein L (hnRNPL) increased DGK-α expression and partially, but significantly, interfered with the negative effects of miR-297 on cancer cell survival. This report identifies miR-297 as a regulator of cancer cell survival downstream of hypoxia via the targeting of DGK-α, with potential therapeutic implications.

Materials and Methods

Cell Culture

Glioma cell lines U87, A172, and T98G were acquired from American Type Culture Collection, and the human telomerase reverse transcriptase–immortalized human astrocyte cell line was a kind gift from Dr Russell Pieper (University of California, San Francisco). U251 glioma was a gift of Dr Howard Fine (New York University Langone Medical Center). GBM stem cell lines 0308, 0822, and 1228 were gifts of Dr Jeongwu Lee (Cleveland Clinic) and have been previously published and characterized.[26] All cell lines were grown under previously described conditions.[8–10]

Materials

Pre-miR control and pre–miR-297 were obtained from Applied Biosystems/Ambion. Control and miR-297–specific inhibitors were obtained from Dharmacon RNA Technologies. Control and DGK-α small interfering (si)RNA were obtained from Sigma.The DGK-α siRNA sequence was: 5′GGAUUGACCCUGUUCCUAA3′. HnRNPL siRNA and control were obtained from Santa Cruz Biotechnology.

Transfection of Cells

MiRNAs and siRNAS were transfected into cells using Oligofectamine (Invitrogen) reagent as previously described.[10,27] All plasmid transfections were carried out using X-tremeGENE HP (Roche Diagnostics). For luciferase assay of wild-type or mutant outputs of DGK-α 3′UTR reporter (Origene), cells were first transfected with control pre-miR or pre–miR-297 and 6 h later were transfected with 1.0 μg wild-type or mutant DGK-α 3′UTR reporter or control empty luciferase plasmid plus 0.05 μg cytomegalovirus–β-galactosidase (or in some experiments together with empty plasmid vector or hnRNPL plasmid) (a kind gift of Dr Paul L. Fox of the Lerner Research Institute, Cleveland) and incubated at 37°C in normoxic (21% pO_2) or hypoxic (1% pO_2) conditions.

Real-time PCR

For the determination of levels of miR-297, patient samples were obtained from the University of Virginia Neuro-Oncology Tumor Bank (with approval from the university's institutional review board), or cells were appropriately transfected or transduced, cultured for several days, and lysed using Qiazol and QIAshredder columns (Qiagen). RNA was isolated using the Qiagen miRNeasy kit. Real-time (RT)–PCR on 500 ng of RNA using the miScript reverse transcription kit (Qiagen) was used to generate cDNA. From 60–96 ng of cDNA template, quantitative (q)RT-qPCR analysis was performed using miR-297- and U6B-specific forward primers and a universal reverse primer according to Qiagen protocol. U6B was used as a control to normalize the levels of miR-297. DGK-α primers were obtained and previously described as referenced,[28] and hnRNPL primers were obtained from Qiagen and compared with the housekeeping gene 18S as previously described.[29] The StepOnePlus RT-PCR system (Applied Biosystems) was used to carry out qPCR. Data analysis for the differences in miR-297 expression was carried out using StepOne Software v2.1 (Applied Biosystems) and Microsoft Excel 2010.

Determination of Cell Numbers (Cell Count)

Cells transfected with either control pre-miR or pre–miR-297 were cultured for 2–3 days. The number of cells was determined by microscopy (Zeiss Axiovert 40C) via hemocytometer using trypan blue exclusion.[8] AlamarBlue was used during preliminary assays to determine that live cell numbers correlated strongly with cellular respiration/metabolism.

Protein Extraction and Quantification

Cells were lysed in 1X cell lysis buffer containing 0.2% sodium dodecyl sulfate (SDS) and protease inhibitors (Cell Signaling Technology). Protein assay was performed using bovine serum albumin as a standard and quantified using the bicinchoninic acid kit according to Bio-Rad protocol. The protein concentrations of samples were calculated as previously described.[8] In experiments involving SDS–polyacrylamide gel electrophoresis, an equal protein concentration of each sample was loaded.

Immunoblots

Immunoblots were performed as previously described.[8–10,27] Primary antibodies included mouse anti–α-tubulin

(11H10) and rabbit polyclonal immunoglobulin G antibody directed against DGK-α (Protein Tech Group) and anti–poly(ADP-ribose) polymerase (PARP; Cell Signaling Technology). Horseradish peroxidase–conjugated secondary antibodies to rabbit or mouse immunoglobulin G were used (Jackson Immunology Labs).

Flow Cytometry Analysis of Apoptosis

Cells were fixed and stained with propidium iodide (Sigma) as previously described.[9] Apoptosis flow cytometry analysis was performed on an ImageStream system (Amnis), which allows the visual capture of individual cell nuclei and performs analysis of DNA fragmentation.

Caspase-3/-7 Assay

Cells transfected with either control pre-miR or pre–miR-297 were detached with the aid of trypsin and suspended in 100 μL phosphate buffered saline. Caspase-3/-7 activity was quantified as previously described.[8,27]

Luciferase Assay

Luciferase reporter assays were performed as previously described.[27] Wild-type or mutant DGK-α 3′UTR luciferase activities were normalized by dividing luciferase activity in each well by β-galactosidase. Fold change in luciferase output was computed as previously described.[8,27]

Cell Invasion Assay

T98G and U251 cells were transfected with either control pre-miR or pre–miR-297 and cultured for 24 h. The cells were detached and counted, and equal numbers of cells were subjected to invasion assay using the modified Boyden chamber (Becton Dickson) as previously described, with staining with crystal violet 0.05% and removal of the cells on the top of the chamber using a tissue after 8 h of incubation on the type IV collagen–coated membrane.[8]

Tumor Formation In vivo

U251 cells were transfected with control pre-miR or pre–miR-297 for 24 h. The transfected cells were then counted, and 3×10^5 cells were stereotactically (Stoelting) implanted into the right corpus striatum of severe combined immunodeficient (SCID)/NCr Bagg albino (BALB)/c adult male mice ($n = 4$ for each condition).

Alternatively, pCDH-511B vector encoding miR-297 or control sequence was ordered from System Biosciences, and 293 T cells were transfected with the pPACKH1 lentiviral vector packaging system. Viral supernatants were collected at several time points posttransfection and were concentrated using a 5X Peg-It solution for 24–48 h. Concentrated viral particle pellets were resuspended after centrifugation according to protocol directions in sterile 1X phosphate buffered saline and titered using a lentiviral qPCR titration kit (Applied Biomedical Materials). Viral titration was also performed in vitro to determine specificity of miR-297 toxicity, and 1×10^6 particles were injected into SCID/NCr BALB/c adult male mice ($n = 9$ per group) 1 week following inoculation with 25 000 GBM stem cells (1228) essentially as we have described. Quantitative RT-PCR was performed essentially as we have described to assess levels of miR-297 post-infection in vitro, using both control-vector-infected cells and uninfected cells as controls, and with either no polybrene or 1 : 2000 polybrene at the time of infection (results were essentially the same for polybrene and no polybrene controls, but polybrene was toxic to 1228 cells; data not shown).

Cerebral MRI was performed on anesthetized mice at 2 weeks for the U251 mice and at 4 weeks for the 1228 mice, as previously described, and tumor volume was calculated from 3 representative tumor-containing images and averaged as previously described.[9]

Hypoxia Rescue of MiR-297

T98G cells were plated in 6-well plates overnight and then transfected with either 20 nM of control pre-miR or pre–miR-297 for 6 h. They were further cultured for a total time of 48 h at 37°C in normoxic (21% pO_2) or hypoxic (1% pO_2) conditions. For survival assay, cells were detached using trypsin and counted with the aid of a hemocytometer, using trypan blue exclusion. For western blot, cell extracts were performed as detailed previously[30,31] and subjected to immunoblot analysis.

DGK-α and HnRNPL Rescue of MiR-297

Cells were plated and allowed to adhere overnight and were then transfected with either 20 nM of control pre-miR or pre–miR-297 for 6 h. They were then either transfected with 0.5 μg of full-length DGK-α lacking 3′UTR (Invitrogen) or control or hnRNPL plasmid and further cultured for a total time of 48 h. For survival assay, cells were detached using trypsin and counted with the aid of a hemocytometer, using trypan blue exclusion. For western blot, cell extractions were performed as detailed previously[30,31] and subjected to immunoblot analysis.

Statistical Analysis of Data

Data presented in figures as graphs were from a minimum of 3 independent experiments and expressed as standard ± SEM. For calculating statistically significant differences between groups of data, Student's 2-way unpaired *t*-tests were used. For multiple comparisons, a 1-way ANOVA with Bonferroni' posttest was used. For in vivo Kaplan–Meier survival analysis in the lentiviral treatment study, survival times were recorded in GraphPad Prism 5.00 for Windows, and mice with ulcerated scalps or lack of internal tumor growth were censored (2 mice were censored from the control group, 1 from the miR-297 group). Log-rank (Mantel–Cox) and Gehan-Breslow-Wilcoxon tests were performed to assess significance.

Results

Expression of MiR-297 and Its Endogenous Role in Glioblastoma

Previous studies, including ours, have shown that the expression of numerous miRNAs is dysregulated in cancers such as glioblastoma.[3,9–11,32] To investigate the expression pattern of miR-297 in glioblastoma, we measured the levels of this microRNA in glioblastoma patient samples and compared it with normal brain samples using qPCR, whose measurements revealed lower levels of miR-297 in the patient samples versus normal brain (Fig. 1A). However, the differences in the levels of miR-297 between the 2 conditions did not attain statistical significance ($P < .07$; Fig. 1A).

Since we noticed some residual amount of miR-297 in glioblastoma (Fig. 1A), we assessed whether endogenous miR-297 might play a role in the viability of these cells. We therefore transfected U251 and T98G glioblastoma cell lines with either miR-297 inhibitor or control oligonucleotide and assessed their viability. U251 and T98G glioblastoma cell lines transfected with miR-297 inhibitor exhibited a significant increase in numbers compared with control miR inhibitor-transfected cells (Fig. 1B). This suggests that despite the trend toward decreased expression of miR-297 in glioblastoma, it remains a physiologically relevant endogenous regulator of survival and proliferation.

miR-297 Decreases the Survival of Cancer Cells

To test for the phenotypic effects of miR-297 overexpression, we transiently transfected glioblastoma cell lines and measured their viability. Glioblastoma cell lines expressing pre–miR-297 exhibited a significant decrease in their numbers compared with control pre-miR transfected cells as well as untreated and Oligofectamine-treated cells (Fig. 2A–B and Fig. 5, Supplemental Fig. 1A and B). We also observed decreased cell viability through alamarBlue and confirmed overexpression of miR-297 in transfected cells (Supplemental Fig. 1C-D). In contrast, human brain astrocytic cells transfected with pre–miR-297 exhibited little decrease in numbers (Fig. 2A). Pre–miR-297 was cytotoxic for glioblastoma stem cell lines, with the greatest effect observed in the GSC-1228 line (Fig. 2B).

We then determined the effects of miR-297 on the induction of apoptosis in glioblastoma by measuring caspase-3/-7 activation, PARP cleavage, and DNA fragmentation—3 well-known hallmarks of apoptosis.[30,33] Caspase-3/-7 activation was measured using luminometry, PARP cleavage by immunoblot, and DNA fragmentation by flow cytometry (Fig. 2C–F). There was a significant increase in the combined activities of caspase-3 and -7 in U251 and T98G cell lines transfected with pre–miR-297 compared with cells transfected with control pre-miR (Fig. 2C). We also observed an increase in the cleavage of PARP from the active 116-kda DNA repair molecule to the inactive 89-kda molecule (Fig. 2D).[34,35] Flow cytometry analysis of U251 and T98G cell lines transfected with pre–miR-297 and stained with propidium iodide revealed an increase in the percentage of cells with fragmented nuclei, with representative images of U251 shown (Figs. 2E and F). In contrast, cells transfected with control pre-miR had little or no nuclei that were fragmented (Fig. 2E and F). These data show that miR-297 induced an apoptotic cell death in glioblastoma lines and may have relevance as a tumor suppressor in other cancer types.

Effects of MiR-297 on Glioblastoma Tumorigenicity

Since miR-297 induced the activation of caspase-3/-7, increased PARP cleavage, and DNA fragmentation (apoptosis) of glioblastoma cells, we hypothesized that this miRNA would suppress the tumorigenic potential of these cell lines. To investigate this possibility, we first quantified the ability of U251 and T98G cell lines to invade through collagen IV–coated transwells, a well-known in vitro assay of tumorigenic invasiveness. This assay was performed 24 h after the transfection of the cancer cell lines with either control pre-miR or pre–miR-297, a time point at which the difference in cell viability has not yet emerged, and invasion was allowed to proceed for 8 h.

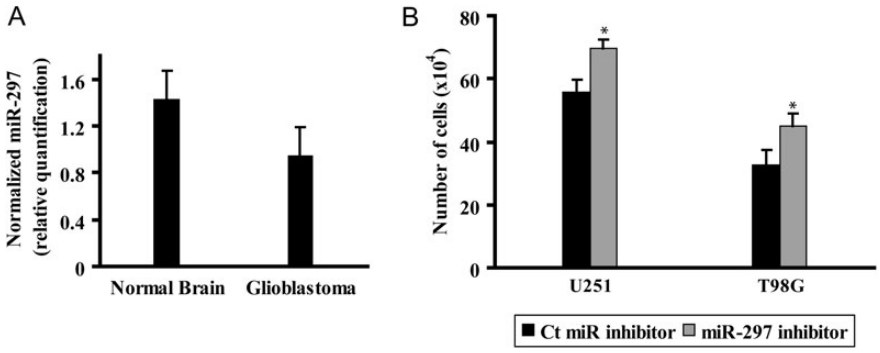

Fig. 1. miR-297 has tumor-suppressive properties in glioblastoma cells. (A) Plot of mRNA expression of mature miR-297 in 12 glioblastoma samples relative to 4 samples taken from normal brain performed by qPCR and normalized with U6B siRNA. (B) Plots of cell counts performed 72 h after the transfection of T98G and U251 glioblastoma cells with either control miR inhibitor (Ct miR inhibitor) or miR-297 inhibitor (*$P < .05$).

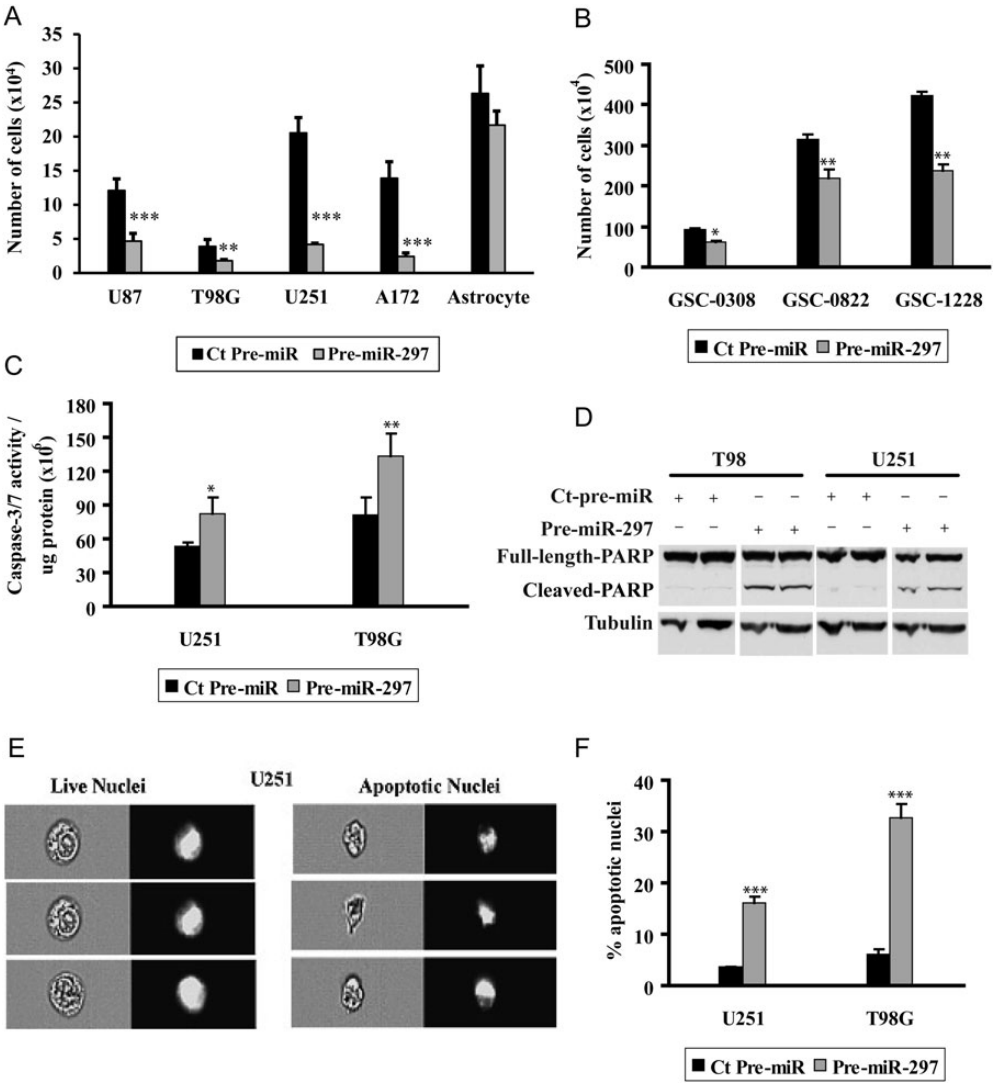

Fig. 2. miR-297 induces the apoptosis of cancer cells. (A) Plots of cell counts performed 72 h after the transfection of T98G, U251, U87, and A172 glioblastoma cells, as well as transformed human astrocyte cells or 3 glioblastoma stem cell lines (B) with either control pre-miR (Ct pre-miR) or pre–miR-297 (***$P < .001$; **$P < .01$; *$P < .05$). (C) Plot of caspase-3 and -7 activities normalized with protein concentration in T98G and U251 glioblastoma cells 48 h after transfection with either control pre-miR (Ct pre-miR) or pre–miR-297 (**$P < .01$ and **$P < .05$). (D) Immunoblots of full-length and cleaved PARP protein in T98G and U251 glioblastoma cells 72 h after transfection with either control pre-miR (Ct pre-miR) or pre–miR-297. Bottom, tubulin as loading control. (E) U251 glioblastoma cells were transfected with either control pre-miR (Ct pre-miR) or pre–miR-297, stained with propidium iodide, subjected to flow cytometry, and presented as a photomicrograph of live or apoptotic nuclei and (F) plot of quantified apoptotic nuclei for both U251 and T98G (***$P < .001$).

U251 and T98G glioblastoma cell lines transfected with pre–miR-297 exhibited significantly reduced invasive ability through collagen matrix compared with control pre-miR–transfected cells (Fig. 3A–C).

Secondly, we tested the ability of U251 glioblastoma cells bearing miR-297 to form tumors in the brains of immunocompromised mice. All mice ($n = 4$) stereotactically implanted with control pre-miR–transfected U251 cells developed large tumors within 2 weeks, while all animals ($n = 4$) bearing U251 cells transfected with pre–miR-297 had barely detectable tumors (Fig. 3D and E). These data suggest that miR-297 suppresses the invasive and tumor-forming properties of glioblastoma cells.

We next validated the GBM stem cell toxicity of miR-297 by infecting GBM stem cells (GSC-1228) with a lentiviral vector containing miR-297 and performing in vitro analyses of viral efficacy prior to xenograft. Decreased alamarBlue fluorescence, increased dead cell numbers, and increased miR-297 are shown in miR-297–transduced cells compared with empty vector–transduced cells (Supplemental Fig. 2A–C). Increased miR-297 expression was observed within 4 days of transduction, and reduced alamarBlue and increased dead cells were observed 6 days after transduction. Mice inoculated with 1228 were then treated with lentivirus after the tumor was established ($n = 9$ per group), and MRI showed that

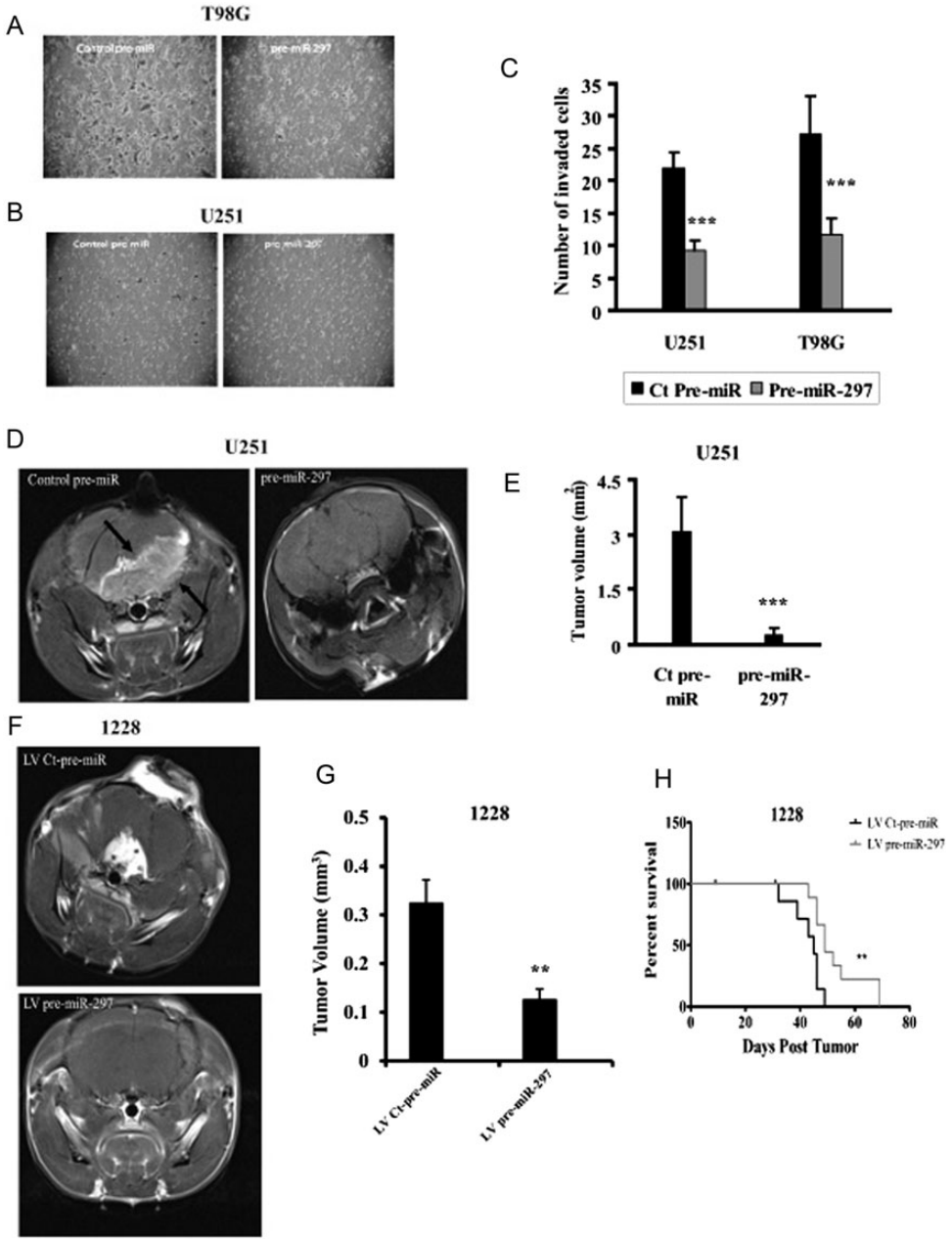

Fig. 3. miR-297 blocks the tumorigenic potential of glioblastoma cells. T98G and U251 cells were transfected with either control pre-miR or pre–miR-297 for 24 h and subsequently subjected to a modified Boyden chamber invasion assay. The assay determines the number of invaded cells through collagen matrix. The data are presented as (A and B) photomicrographs of invaded cells and (C) a plot of the number of invaded cells. (D) Representative brain MRIs in mice bearing U251 glioblastoma cells in the control pre-miR group compared with the pre–miR-297 group. (E) The mean tumor sizes were plotted (***$P < .001$). (F) Representative brain MRIs in mice bearing 1228 glioblastoma stem cells, with control and miR-297 lentiviral vector treatments, with mean tumor sizes plotted (**$P < .01$). (G and H) Tumor survival Kaplan–Meier analysis for lentiviral control and pre–miR-297 groups (**$P < .01$).

miR-297 overexpression resulted in decreased tumor volume and increased survival (Fig. 3F–H).

MiR-297 Acts in Part via Targeting DGK-α Through Its 3′UTR

To investigate potential targets explaining the cytotoxicity of miR-297, we searched multiple online databases for top predicted targets (Targetscan, MicroCosm, microRNA.org). Notably, there were no established oncogenes among them. However, we observed that one of the top predicted targets, DGK-α, had been linked in previous reports to the activity of several pathways implicated in cancer.[36,37] We recently published a report further elucidating DGK-α's potential as a target in several cancers.[28] Targetscan revealed 2 potential sites for miR-297 in the DGK-α 3′UTR (Fig. 4A).

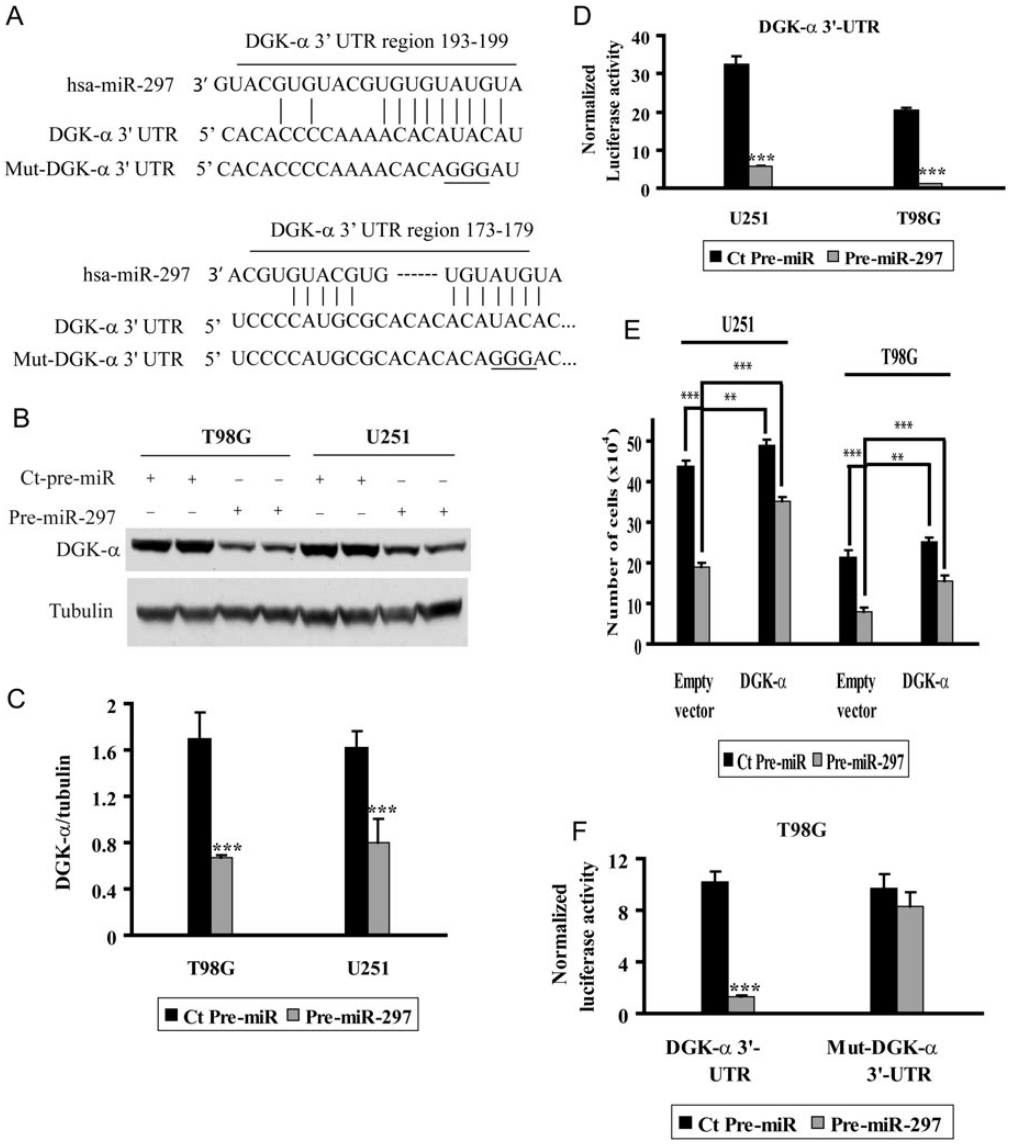

Fig. 4. miR-297 regulation of DGK-α occurs through its 3′UTR. (A) Sites of miR-297 seed matches with or without mutations in 3 bases (TAC changed to GGG). (B) Immunoblot showing protein expression of DGK-α in U251MG and T98G cells, 2 days after transfection with either control pre-miR (Ct pre-miR) or pre–miR-297 (tubulin loading controls shown at bottom). (C) Several representative immunoblots of DGK-α expression as in (B) are quantified, normalized with quantified tubulin, and presented as a bar graph (***$P < .001$). (D) Normalized activity of DGK-α 3′UTR luciferase reporter plasmid 2 days after the transfection of T98G and U251 cells with either control pre-miR or pre–miR-297 (***$P < .001$). (E) Plots of cell counts performed 72 h after the transfection of T98G and U251 glioblastoma cells with either control pre-miR (Ct pre-miR) or pre–miR-297 together with either empty control plasmid vector or plasmid bearing DGK-α protein lacking 3′UTR (***$P <$ .001 and **$P < .01$). (F) Normalized activity of wild-type or mutant DGK-α 3′UTR luciferase reporter plasmid 2 days posttransfection of T98G cells with either control pre-miR (Ct pre-miR) or pre–miR-297 (***$P < .001$).

Immunoblot analysis of glioblastoma cell lines transfected with pre–miR-297 revealed significantly lower levels of DGK-α protein but not mRNA compared with cells bearing control pre-miR or untreated or Oligofectamine-treated controls (Fig. 4B and C, Supplemental Fig. 3A–E).

To test whether miR-297 acts directly on the DGK-α 3′UTR, we tested its effects on a luciferase/DGK-α 3′UTR reporter plasmid. Transfection of established glioblastoma cell lines with pre–miR-297 abrogated DGK-α 3′UTR luciferase output (Fig. 4D). miR-297 has other predicted targets besides *DGKA* (Targetscan), and some of them could be functionally relevant to the cytotoxic effects of miR-297. To determine whether the inhibition of DGK-α protein expression could play a role in the cytotoxic effects of miR-297, we tested the ability of DGK-α restoration to prevent miR-297–induced glioblastoma cell death. We noted that the transfection of T98G and U251 glioblastoma cell lines with a DGK-α plasmid lacking its 3′UTR significantly rescued miR-297–induced cytotoxic effects (Fig. 4E). To confirm the physiological

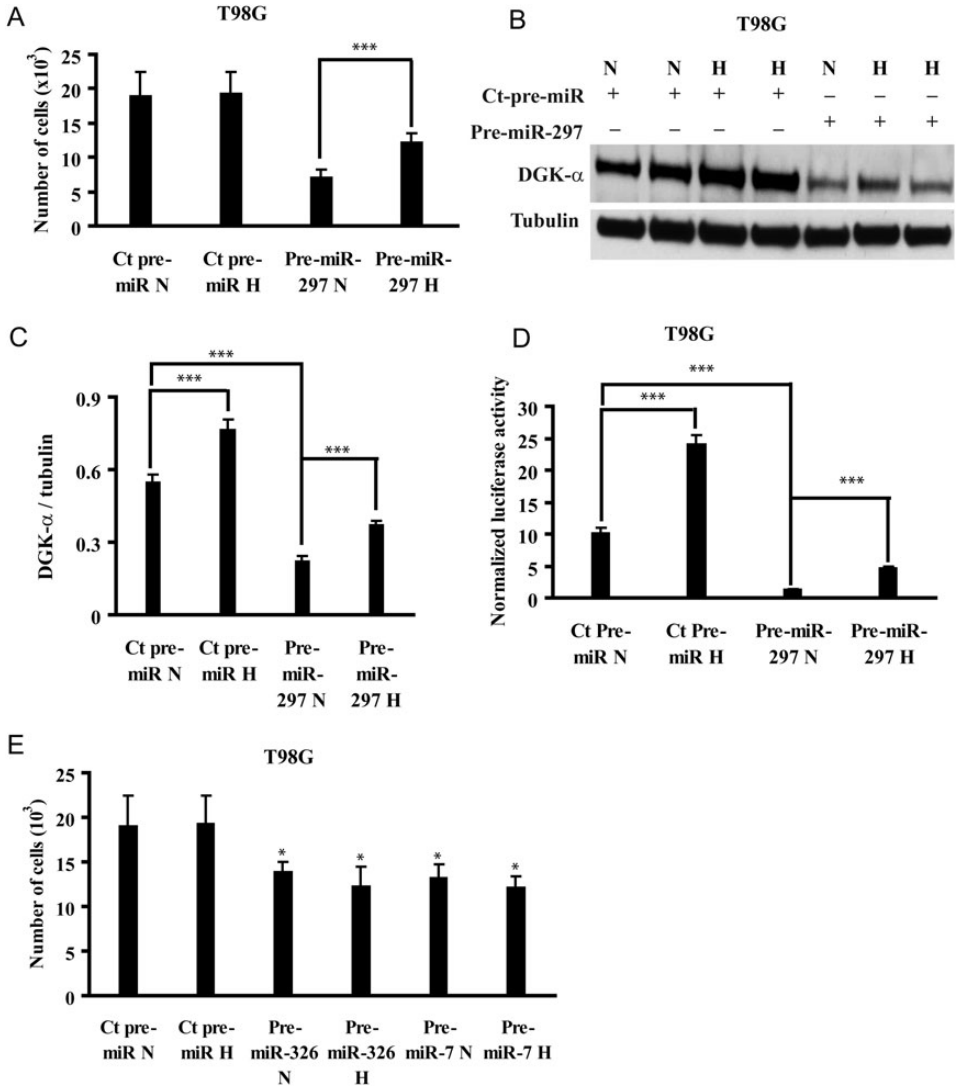

Fig. 5. Hypoxia buffers effects of miR-297 on cancer cells. (A) Plots of cell counts performed 48 h after the transfection of T98G glioblastoma cells with either control pre-miR (Ct pre-miR) or pre–miR-297 and exposure to either hypoxic (H) or normoxic (N) conditions (***$P < .001$). (B) Immunoblots showing the protein expression of DGK-α in T98G glioma cells 2 days post treatment with either control pre-miR (Ct pre-miR) or pre–miR-297 and exposure to either normoxic (N) or hypoxic (H) conditions (tubulin as loading control shown at the bottom). (C) Three repeated experiments as in (B) are quantified and presented as a bar graph (***$P < .001$). (D) Normalized activity of DGK-α 3′UTR luciferase reporter plasmid 2 days after transfection of T98G glioblastoma cells with either control pre-miR (Ct pre-miR) or pre–miR-297 and exposure to either normoxic (N) or hypoxic (H) conditions (***$P < .001$). (E) Plots of cell counts performed 48 h after the transfection of T98G glioblastoma cells with either control pre-miR (Ct pre-miR) or pre–miR-326 or pre–miR-7 and exposure to either hypoxic (H) or normoxic (N) conditions (*$P < .05$).

role of DGK-α in the survival of cancer cells, we modulated its expression using specific siRNA. Transfection of glioblastoma cancer cells with a validated DGK-α siRNA significantly reduced both DGK-α protein and cell numbers (Supplemental Fig. 3F–G).[28]

To further confirm the mechanism by which miR-297 regulates DGK-α 3′UTR, we mutated 3 nucleotides each on the 2 miR-297 binding sites in the DGK-α 3′UTR (Fig. 4A). These mutations completely blocked the negative effects of miR-297 on DGK-α 3′UTR luciferase output (Fig. 4F). These data suggest that DGK-α is a direct target of miR-297 and that regulation of DGK-α protein by miR-297 is through its binding and inhibition of the DGK-α 3′UTR. The results also indicate DGK-α suppression as a mediator of miR-297 effects.

Hypoxia Buffers Cytotoxicity of MiR-297 in Glioblastoma

A recent study identified hypoxia and the expression of one of its mediators, the RNA binding protein hnRNPL, as variables that interfered with the effects of miR-297 and other microRNAs targeting vascular endothelial

growth factor A (*VEGFA*).[25] We predicted that these conditions would also affect miR-297 effects on DGK-α and the cytotoxic effects of miR-297 in cancer cells. To test this for hypoxic conditions, we transfected a T98G glioblastoma cell line with either control pre–miR or pre–miR-297 and cultured them in either normoxic or hypoxic conditions for 48 h. miR-297 significantly decreased the number of T98G cells cultured in normoxic conditions compared with control pre-miR–transfected cells (Fig. 5A). Notably, hypoxic conditions partially but significantly blocked the cytotoxic effects and targeting of DGK-α protein levels and the 3′UTR by miR-297 in T98G (Fig. 5A–D). Hypoxia had no effect on the cytotoxicity of 2 other tumor-suppressive microRNAs we have described previously (Fig. 5E).

HnRNPL Upregulates DGK-α Levels Through the Modulation of the DGK-α 3′UTR

Given that hypoxia ameliorated the cytotoxic effects of miR-297 (Fig. 5A),[25] we hypothesized that hnRNPL would specifically influence DGK-α expression given its known effect on other targets of miR-297. In addition, we identified putative hypoxia (C/CTT/CC/C and TCCCCT) and hnRNP L (CA) regulatory elements in the DGK-α 3′UTR (Figs. 4A and 6A),[19,20,25,38–41] suggesting that both hypoxia and hnRNPL might alter the levels of DGK-α and interfere with the effects of miR-297 on the DGK-α 3′UTR.

To test the effect of hnRNPL overexpression on DGK-α expression, T98G cells were transfected with

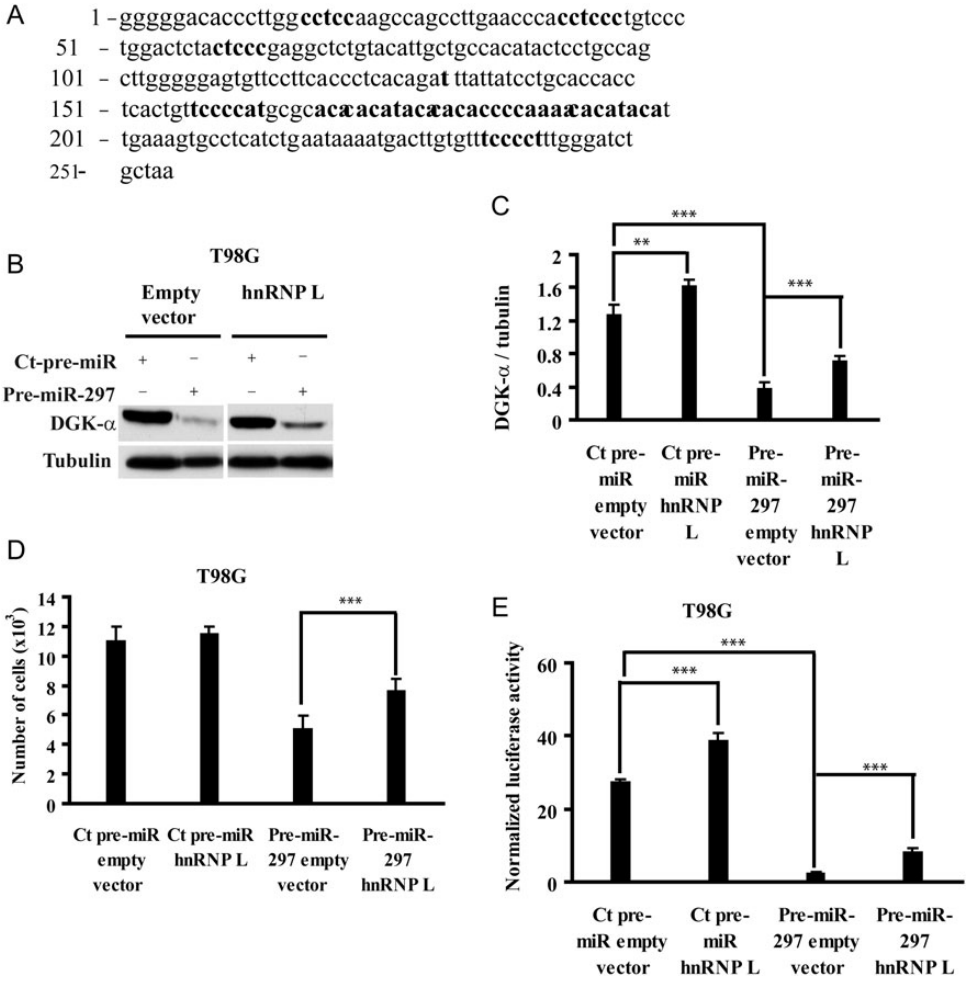

Fig. 6. HnRNPL blocks the effects of miR-297 through the upregulation of DGK-α expression. (A) Predicted CA-rich region binding sites for hnRNPL and predicted hypoxia-inducible sites highlighted (CCTCC, CTCCC, CCTCCC; nucleotides 16–20, 39–44, and 115–125, T/ACCCCT/A; nucleotides 158–161, 181–186, and 235–241)[18,20,21,38–41] in the DGK-α 3′UTR. (B) Immunoblot showing the protein expression of DGK-α in T98G glioma cells 2 days posttreatment with either control pre-miR or pre–miR-297 together with either control plasmid vector or plasmid bearing hnRNPL. (C) Three repeated experiments as in (B) are quantified and presented as a bar graph (***$P < .001$ and **$P < .01$). (D) Plots of cell counts performed 48 h after the transfection of T98G glioblastoma cells with either control pre-miR (Ct pre-miR) or pre–miR-297 together with either empty control plasmid vector or plasmid bearing hnRNPL gene (***$P < .001$). (E) Normalized activity of DGK-α 3′UTR luciferase reporter plasmid 2 days after transfection of T98G glioblastoma cells with either control pre-miR or pre–miR-297 together with control empty vector plasmid or plasmid bearing hnRNPL gene (***$P < .001$).

control pre–miR or pre–miR-297, together with either control plasmid or plasmid bearing the hnRNPL gene. We quantified DGK-α protein levels using immunoblot and the regulation of its 3′UTR using a luciferase reporter plasmid. HnRNPL overexpression significantly upregulated both DGK-α protein and 3′UTR reporter activity (Fig. 6B, C, and E) and partially but significantly prevented the inhibitory effects of miR-297 on these readouts (Fig. 6B, C, and E).

To test whether hnRNPL could prevent miR-297 cytotoxicity in glioblastoma cells, we transfected T98G cell lines with either control pre–miR or pre–miR-297, together with either control or hnRNPL plasmid and performed cell counts. We observed a partial rescue of miR-297–mediated cell number decrease in T98G cells overexpressing hnRNPL compared with control plasmid (Fig. 6D). We confirmed hnRNPL overexpression and knockdown with qPCR and tested the effect of hnRNPL siRNA on T98 cell viability in hypoxic and normoxic conditions (Supplemental Fig. 4A–D). The death of more than 50% of the cells in the hnRNPL siRNA + hypoxia group was surprising. These data suggest that DGK-α is a functional target of miR-297 and that hypoxic conditions and the hypoxic mediator hnRNPL partially but significantly interfere with the cytotoxic effects of miR-297 in glioblastoma. While we did see a potential decrease in DGK-α expression with hnRNPL siRNA in hypoxic conditions, the cytotoxicity in both normoxia and hypoxia induced by hnRNPL siRNA made conclusions about DGK-α expression difficult (SF4). Our findings suggest that DGK-α is a hypoxia-regulated gene and indicate that hypoxia and hnRNPL modulate miR-297 effects.

Discussion

These results establish miR-297 as a potential tumor-suppressive miRNA, with substantial cytotoxic effects in glioblastoma cells and minimal effects in normal cells. That being considered, miR-297 expression does not seem to be markedly downregulated in glioblastoma by standard mechanisms such as deletion; however, we have found that the cytotoxic effects of miR-297 can be dampened in cancer cells by a mechanism prevalent in tumors: hypoxia. Hypoxia has previously been shown to promote the relocation of hnRNPL from the cell nucleus to the cytosol, where it may not only block the effects of miR-297 on its target but also stabilize RNA transcripts.[20] While this still leaves a baseline level of miR-297 activity in cancer cells, it also permits regulated buffering of miR-297 toxicity.

One implication of this study is the potential of miR-297 delivery as a therapy for glioblastoma and other cancers. A number of tumor-suppressive microRNAs have been reported, and while efficient delivery remains problematic, there is progress being made on this front—including in the current study—where we show effective lentiviral delivery of miR-297 to a xenograft that results in increased survival. One caveat suggested by these results is that cancer cells in regions of hypoxia may be partially protected from the effects of miR-297 delivery. However, our data suggest that forced overexpression of miR-297 appears able to drive substantial cancer cell death even in hypoxic conditions.

The miR-297 target DGK-α has not received significant attention as a target in cancer. However, prior reports, including our own recently published work,[28] have shown a striking association of DGK-α with numerous oncogenic pathways, including Ras/Raf, Akt/mammalian target of rapamycin (mTOR)C1/mTORC2, hypoxia-inducible factor–1α, c-Met, anaplastic lymphoma kinase, and VEGF.[36,42–45] While we identify DGK-α as an important target of miR-297, the partial rescue of GBM cell numbers with DGK-α expression suggests that other relevant targets of this miRNA have yet to be identified.

Our investigations of hypoxia and the RNA-binding protein hnRNPL as modulators of miR-297 cytotoxic effects were prompted by a recent report indicating their influence on VEGFA targeting by miR-297 and 2 other miRNAs.[25] That report showed that hypoxia elevated the expression of hnRNPL in cellular cytosol, which bound the VEGFA 3′UTR at loci overlapping the binding sites for miR-297 and the other miRNAs—thus blocking the miRNAs and elevating VEGFA expression.[25] We noted the possibility that the same mechanism might also apply to miR-297 targeting of DGK-α, and this was supported by our results. It should be noted that another mechanism may also contribute to hypoxic regulation of DGK-α expression. The DGK-α 3′UTR appears to contain domains that have been termed "hypoxia stability regions," which allow hypoxic upregulation of these genes by unknown mechanisms.[19,20,25,38–41] Regardless of the relative contributions by these mechanisms, it is clear that hypoxia and hnRNPL modulate DGK-α expression and thus the effects of miR-297 on glioblastoma survival.

In conclusion, this work establishes miR-297 as a hypoxia-modulated physiologic regulator of cancer cell survival with both biologic and therapeutic implications. It is tempting to speculate that modulation of miR-297 effects may also partially mediate the effects of hypoxia on glioblastoma and other cancer cells; the dampening of miR-297 cytotoxicity may represent one mechanism by which hypoxia promotes cancer cell survival.

Supplementary Material

Supplementary material is available online at *Neuro-Oncology* (http://neuro-oncology.oxfordjournals.org/).

Acknowledgments

We would like to thank Dr Paul L. Fox of the Lerner Research Institute, Cleveland, OH, for the generous gift of the hnRNPL plasmid.

Conflict of interest statement. None declared.

Funding

This work was supported by NIH R01CA136803 (B.P.).

References

1. Raguz S, Yague E. Resistance to chemotherapy: new treatments and novel insights into an old problem. *Br J Cancer*. 2008;99(3):387–391.
2. Vogelstein B, Kinzler KW. Cancer genes and the pathways they control. *Nat Med*. 2004;10(8):789–799.
3. Chan JA, Krichevsky AM, Kosik KS. MicroRNA-21 is an antiapoptotic factor in human glioblastoma cells. *Cancer Res*. 2005;65(14):6029–6033.
4. Corsten MF, Miranda R, Kasmieh R, Krichevsky AM, Weissleder R, Shah K. MicroRNA-21 knockdown disrupts glioma growth in vivo and displays synergistic cytotoxicity with neural precursor cell delivered S-TRAIL in human gliomas. *Cancer Res*. 2007;67(19):8994–9000.
5. Cui JG, Zhao Y, Sethi P, et al. Micro-RNA-128 (miRNA-128) down-regulation in glioblastoma targets ARP5 (ANGPTL6), Bmi-1 and E2F-3a, key regulators of brain cell proliferation. *J Neurooncol*. 2010;98(3):297–304.
6. Duex JE, Comeau L, Sorkin A, Purow B, Kefas B. Usp18 regulates epidermal growth factor (EGF) receptor expression and cancer cell survival via microRNA-7. *J Biol Chem*. 2011;286(28):25377–25386.
7. Hulleman E, Helin K. Molecular mechanisms in gliomagenesis. *Adv Cancer Res*. 2005;94:1–27.
8. Kefas B, Comeau L, Erdle N, Montgomery E, Amos S, Purow B. Pyruvate kinase M2 is a target of the tumor-suppressive microRNA-326 and regulates the survival of glioma cells. *Neuro Oncol*. 2010;12(11):1102–1112.
9. Kefas B, Comeau L, Floyd DH, et al. The neuronal microRNA miR-326 acts in a feedback loop with notch and has therapeutic potential against brain tumors. *J Neurosci*. 2009;29(48):15161–15168.
10. Kefas B, Godlewski J, Comeau L, et al. microRNA-7 inhibits the epidermal growth factor receptor and the Akt pathway and is down-regulated in glioblastoma. *Cancer Res*. 2008;68(10):3566–3572.
11. Li Y, Guessous F, Zhang Y, et al. MicroRNA-34a inhibits glioblastoma growth by targeting multiple oncogenes. *Cancer Res*. 2009;69(19):7569–7576.
12. Zhang Y, Chao T, Li R, et al. MicroRNA-128 inhibits glioma cells proliferation by targeting transcription factor E2F3a. *J Mol Med*. 2009;87(1):43–51.
13. Bartel DP. MicroRNAs: genomics, biogenesis, mechanism, and function. *Cell*. 2004;116(2):281–297.
14. Murchison EP, Hannon GJ. miRNAs on the move: miRNA biogenesis and the RNAi machinery. *Curr Opin Cell Biol*. 2004;16(3):223–229.
15. Ambros V. The functions of animal microRNAs. *Nature*. 2004;431(7006):350–355.
16. Kim VN. MicroRNA biogenesis: coordinated cropping and dicing. *Nat Rev Mol Cell Biol*. 2005;6(5):376–385.
17. Comprehensive genomic characterization defines human glioblastoma genes and core pathways. *Nature*. 2008;455(7216):1061–1068.
18. Mazurek S, Boschek CB, Hugo F, Eigenbrodt E. Pyruvate kinase type M2 and its role in tumor growth and spreading. *Semin Cancer Biol*. 2005;15(4):300–308.
19. Shih SC, Claffey KP. Hypoxia-mediated regulation of gene expression in mammalian cells. *Int J Exp Pathol*. 1998;79(6):347–357.
20. Claffey KP, Shih SC, Mullen A, et al. Identification of a human VPF/VEGF 3′ untranslated region mediating hypoxia-induced mRNA stability. *Mol Biol Cell*. 1998;9(2):469–481.
21. Spence AM, Muzi M, Swanson KR, et al. Regional hypoxia in glioblastoma multiforme quantified with [18F]fluoromisonidazole positron emission tomography before radiotherapy: correlation with time to progression and survival. *Clin Cancer Res*. 2008;14(9):2623–2630.
22. Liang BC. Effects of hypoxia on drug resistance phenotype and genotype in human glioma cell lines. *J Neurooncol*. 1996;29(2):149–155.
23. Hockel M, Vaupel P. Tumor hypoxia: definitions and current clinical, biologic, and molecular aspects. *J Natl Cancer Inst*. 2001;93(4):266–276.
24. Vaupel P, Kelleher DK, Hockel M. Oxygen status of malignant tumors: pathogenesis of hypoxia and significance for tumor therapy. *Semin Oncol*. 2001;28(2 Suppl 8):29–35.
25. Jafarifar F, Yao P, Eswarappa SM, Fox PL. Repression of VEGFA by CA-rich element-binding microRNAs is modulated by hnRNP L. *EMBO J*. 2011;30(7):1324–1334.
26. Lee J, Kotliarova S, Kotliarov Y, et al. Tumor stem cells derived from glioblastomas cultured in bFGF and EGF more closely mirror the phenotype and genotype of primary tumors than do serum-cultured cell lines. *Cancer Cell*. 2006;9(5):391–403.
27. Purow BW, Haque RM, Noel MW, et al. Expression of Notch-1 and its ligands, Delta-like-1 and Jagged-1, is critical for glioma cell survival and proliferation. *Cancer Res*. 2005;65(6):2353–2363.
28. Dominguez CL, Floyd DH, Xiao A, et al. Diacylglycerol kinase alpha is a critical signaling node and novel therapeutic target in glioblastoma and other cancers. *Cancer Discov*. 2013;3(7):782–797.
29. Floyd DH, Kefas B, Seleverstov O, et al. Alpha-secretase inhibition reduces human glioblastoma stem cell growth in vitro and in vivo by inhibiting Notch. *Neuro Oncol*. 2012;14(10):1215–1226.
30. Kefas BA, Cai Y, Ling Z, et al. AMP-activated protein kinase can induce apoptosis of insulin-producing MIN6 cells through stimulation of c-Jun-N-terminal kinase. *J Mol Endocrinol*. 2003;30(2):151–161.
31. Kefas BA, Heimberg H, Vaulont S, et al. AICA-riboside induces apoptosis of pancreatic beta cells through stimulation of AMP-activated protein kinase. *Diabetologia*. 2003;46(2):250–254.
32. Ciafre SA, Galardi S, Mangiola A, et al. Extensive modulation of a set of microRNAs in primary glioblastoma. *Biochem Biophys Res Commun*. 2005;334(4):1351–1358.
33. Los M, Mozoluk M, Ferrari D, et al. Activation and caspase-mediated inhibition of PARP: a molecular switch between fibroblast necrosis and apoptosis in death receptor signaling. *Mol Biol Cell*. 2002;13(3):978–988.
34. Morrison C, Smith GC, Stingl L, Jackson SP, Wagner EF, Wang ZQ. Genetic interaction between PARP and DNA-PK in V(D)J recombination and tumorigenesis. *Nat Genet*. 1997;17(4):479–482.
35. Wang ZQ, Stingl L, Morrison C, et al. PARP is important for genomic stability but dispensable in apoptosis. *Genes Dev*. 1997;11(18):2347–2358.
36. Baldanzi G, Mitola S, Cutrupi S, et al. Activation of diacylglycerol kinase alpha is required for VEGF-induced angiogenic signaling in vitro. *Oncogene*. 2004;23(28):4828–4838.
37. Topham MK, Prescott SM. Mammalian diacylglycerol kinases, a family of lipid kinases with signaling functions. *J Biol Chem*. 1999;274(17):11447–11450.
38. Ray PS, Jia J, Yao P, Majumder M, Hatzoglou M, Fox PL. A stress-responsive RNA switch regulates VEGFA expression. *Nature*. 2009;457(7231):915–919.
39. Levy AP, Levy NS, Goldberg MA. Hypoxia-inducible protein binding to vascular endothelial growth factor mRNA and its modulation by the von Hippel–Lindau protein. *J Biol Chem*. 1996;271(41):25492–25497.

40. Levy AP, Levy NS, Goldberg MA. Post-transcriptional regulation of vascular endothelial growth factor by hypoxia. *J Biol Chem*. 1996;271(5):2746–2753.
41. Levy AP, Levy NS, Wegner S, Goldberg MA. Transcriptional regulation of the rat vascular endothelial growth factor gene by hypoxia. *J Biol Chem*. 1995;270(22):13333–13340.
42. Aragones J, Jones DR, Martin S, et al. Evidence for the involvement of diacylglycerol kinase in the activation of hypoxia-inducible transcription factor 1 by low oxygen tension. *J Biol Chem*. 2001;276(13):10548–10555.
43. Avila-Flores A, Santos T, Rincon E, Merida I. Modulation of the mammalian target of rapamycin pathway by diacylglycerol kinase-produced phosphatidic acid. *J Biol Chem*. 2005;280(11):10091–10099.
44. Temes E, Martin-Puig S, Aragones J, et al. Role of diacylglycerol induced by hypoxia in the regulation of HIF-1alpha activity. *Biochem Biophys Res Commun*. 2004;315(1):44–50.
45. Cutrupi S, Baldanzi G, Gramaglia D, et al. Src-mediated activation of alpha-diacylglycerol kinase is required for hepatocyte growth factor-induced cell motility. *EMBO J*. 2000;19(17):4614–4622.